

## Effect of active control on the shedding of vorticity in cavity flows

Ludovic Chatellier<sup>1</sup>, Janick Laumonier, Yves Gervais

Laboratoire D'Etudes Aérodynamiques, UMR CNRS 6609,  
Bat. K, 40 Av. du Recteur Pineau, 86022 Poitiers Cedex, France.

**Abstract** Active control of the aeroacoustics of flow-induced oscillations in a rectangular cavity is accomplished using a vibrating plate inserted at the downstream edge of the cavity opening. Particle Image Velocimetry measurements phase-locked on pressure signals are carried out and reveal the dynamics of the mixing layer with and without control. A vortex detection criterion is applied to characterize the effect of control on the shedding of small-scale vortical structures.

### 1 Introduction

In many configurations of high Reynolds number cavity flows, self-sustained oscillations of the mixing layer are clearly governed by a Rossiter-like phenomenology [1]. Here, the development of a turbulent boundary layer ahead of the cavity results in patterns of vorticity organized as diffused structures in the mixing layer [2]. In consequence, well defined coherent structures are not observed at the scale of the mixing layer, as in more favourable cases [3].

However, post-processing of phase-locked PIV measurements in the opening of the cavity has revealed the dynamics of the periodically oscillating mixing layer [4]. Once active control is applied, the convective wave animating the mixing layer sees its shape and amplitude sensibly altered while the radiated sound is either attenuated or amplified [5]. The small scale vortices convected in the mixing layer closely follow these oscillations, it is then of interest to characterize the influence of active control on such structures.

### 1 Experimental apparatus

The experimental device is depicted in Figure 1 and consists in a square section cavity of 5.2:1 lateral aspect ratio mounted on a wing profile and installed in an Eiffel wind tunnel. The grazing flow is turbulent, subsonic, with a maximum Mach number of 0.11, which corresponds to a Reynolds number  $Re_L=3.5 \times 10^5$ .

The active control system is based on a frequency tracking board coupled with a sharp band-pass filter. PIV phase-locking is achieved via a frequency divider, while the control command uses a reconstructed sine wave with manual phase and amplitude adjustments. The actuator consists in a 300 mm  $\times$  30 mm aluminium plate located at the downstream edge of the cavity and placed half-way along the wingspan. The plate is attached to an electromagnetic vibrator which generates a

---

<sup>1</sup> Current address : Laboratoire d'Etude des Phénomènes de Transfert Appliqués au Bâtiment, Pôle Sciences et Technologie, Av. Michel Crépeau, 17024 La Rochelle Cedex 1, France

piston-like motion along the main flow direction. An accelerometer attached to the moving plate is used to record the local vibration level during control. The underlying concept of the control is that a dynamic phasing of the boundary conditions in the impinging region can be used in order to act on the retroaction loop.

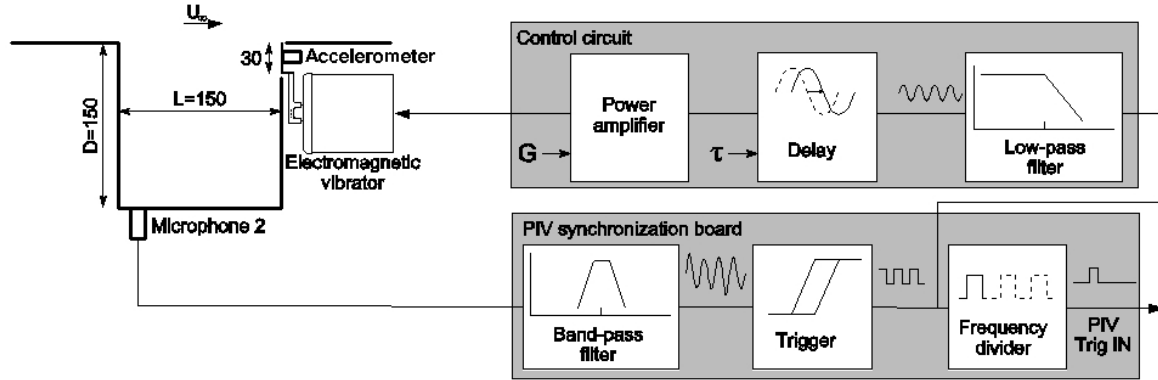


Figure 1: Sketch of the experimental setup

Initially, the phase-locked Particle Image Velocimetry measurements have been conducted so that ten equidistant time lags covering a full cycle of oscillations could be investigated. For each time lag, 100 PIV fields were averaged, revealing that the dynamics of the mixing layer are governed by a convective wave that can be predicted by a linearized model [2]. The same measurement and post-processing methods have been used to characterize the effect of the control on the oscillations of the mixing layer when the control parameters are adjusted to either attenuate or amplify the sound radiated by the cavity in presence of a fluid-resonant aeroacoustic coupling [5].

## 2 Vortex identification

Among other techniques, Jeong and Hussain's vortex criterion [3] has proven to be an efficient indicator of the presence of coherent structures in an incompressible flow. This criterion is given by the second non-zero eigenvalue of the symmetric tensor  $S^2 + \Omega^2$ , where  $S$  and  $\Omega$  are the symmetric and antisymmetric part of the velocity gradient tensor, respectively. In a two dimensional flow, this criterion is equivalent to the  $Q$  criterion and is given by the non-zero local eigenvalue:

$$\lambda = \left( \frac{\partial u}{\partial x} \right)^2 + \frac{\partial v}{\partial x} \frac{\partial u}{\partial y} ,$$

Given an instantaneous or averaged velocity field, this can be used in a very straightforward way as in presence of a vortex, a region of negative  $\lambda$  indicates the extent of its core.

For the simplified case of a two-dimensional isolated vortex of purely tangential velocity, Jeong and Hussain's criterion is expressed by:

$$\lambda = - \frac{\partial v_\theta}{\partial r} \frac{v_\theta}{r} .$$

An exact expression of  $\lambda$  is then available as long as an analytic formulation is used to represent a vortex. For the classically used Lamb-Oseen vortex, the velocity field is:

$$v_r = 0$$

$$v_\theta = \frac{\Gamma}{2\pi r} \left(1 - e^{-r^2/r_0^2}\right) ,$$

and  $\lambda$  is given by

$$\lambda = \frac{\Gamma^2}{\pi^2 r^2} \left[ \frac{1}{r^2} - \left(\frac{1}{r^2} + \frac{2}{r_0^2}\right) e^{-r^2/r_0^2} \right] \left(1 - e^{-r^2/r_0^2}\right) .$$

For the vortex defined in Townsend's example on turbulence statistics [6], the velocity field is given by derivation of a Gaussian stream function  $\Psi = e^{-\frac{1}{2}r^2/r_0^2}$  :

$$u = \frac{-\partial \Psi}{\partial y} = \frac{x}{r_0^2} e^{-\frac{1}{2}r^2/r_0^2}$$

$$v = \frac{\partial \Psi}{\partial x} = \frac{-y}{r_0^2} e^{-\frac{1}{2}r^2/r_0^2} ,$$

which yields for  $\lambda$  :

$$\lambda = \frac{1}{r_0^4} \left( \frac{r^2}{r_0^2} - 1 \right) e^{-r^2/r_0^2} .$$

This slightly simpler formulation is similar in form to the well-known mexican hat wavelet. In terms of pattern recognition using wavelet-like scale filtering, both these results can be applied to isolate vortical patterns.

Vortex identification using Jeong and Hussain's criterion can be efficiently coupled to scale filtering techniques in order to extract position, scale and strength of vortical structures. This type of analysis has been conducted by Öszoj *et. al.* [3] for the specific case of cavity flows , using the mexican hat pattern.

The analysis presented in this paper is based on the filtering of a two-dimensional  $\lambda$  field using a normalized and zero-mean pattern representing a plausible distribution of the  $\lambda$  field in the vicinity of an isolated vortex. Given a discrete range of expected scales at which the analysis is performed, identification of absolute maxima along this third dimension results in a two-dimensional distribution of candidate scales. In practice, such a field obviously contains both valid and non valid scales. However, in this type of distribution, the characteristic signature of a vortex consists in a local minimum of the candidate scales. This property allows detection of valid scales and positions of the corresponding vortices, as shown in Figure 2 for a sample PIV field measured in the mixing layer of the cavity.

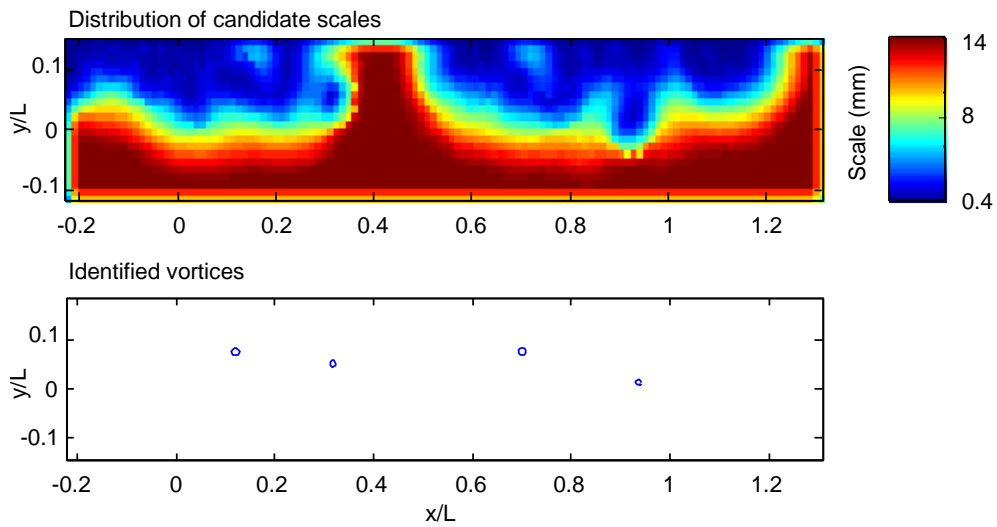


Figure 2: Example of vortex detection from a map of candidate scales

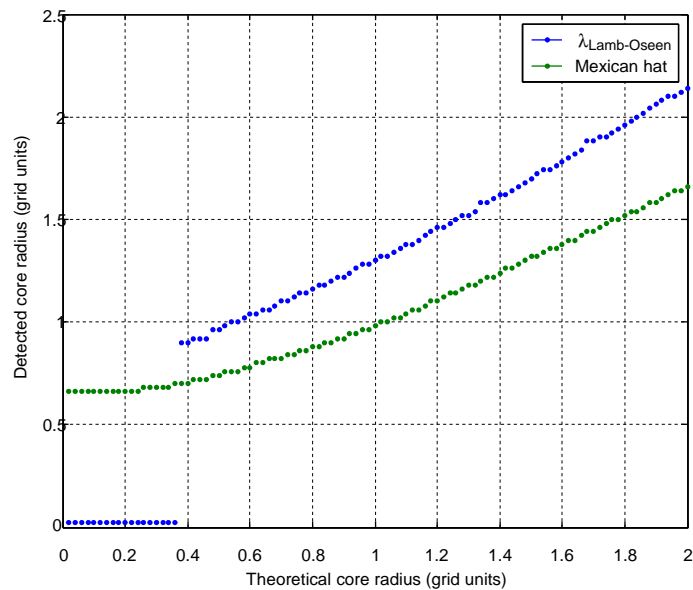


Figure 3: Application of the detection algorithm to small scale Lamb-Oseen vortices

Figure 3 illustrates the sensitivity of the detection algorithm to small variations of the radius of a Lamb-Oseen vortex around the scale of a grid cell. Results from filtering based on the theoretical value of  $\lambda$  and on the mexican hat are compared. At these scales, both forms do not lead to detection of the actual radius of the core, but give a bijective estimation for radii greater than 0.35 and 0.25 grid cells, respectively. In this idealized situation, although the mexican hat form can be used to detect smaller structures, the theoretical  $\lambda$  form gives a slightly higher sensitivity and

logically tends to direct identification of the actual core size at larger scales. It is the very low sensitivity of the mexican hat form at the smallest scales that prevents its use for detection of lower radii, whereas the theoretical form is inefficient below 0.35 grid cells.

### 3 Results

Results obtained from phase-locked PIV have already shown the influence of active control on the periodic oscillations of the mixing layer at a specific mode [5]. It has also been pointed out that large scale vortices are not likely to have a definite influence on the self-sustained modes observed here [2]. Still, the high shear within the mixing layer is responsible for growth of coherent structures, whether they are initially present in the incident boundary layer or not.

Results corresponding to [5] and illustrating the effect of control on the self sustained oscillations of the mixing layer are presented in Figure 4. Flow parameters are as follows:

- $Re_L = 3.4 \times 10^5$  ,
- Mode 3:  $f = 391 \text{ Hz}$  ;  $St = 2$  .

The oscillations reconstructed from the phase-locked PIV measurements are fitted in phase and amplitude to the theoretical convective wave identified in [2]. The perturbing effect of control in the impingement region and around  $x/L = 0.65$  should be retained for comparison with the following results. Similarly, the apparent resurgence of an out-of-phase mode in the first quarter of the controlled mixing layer should be noted.

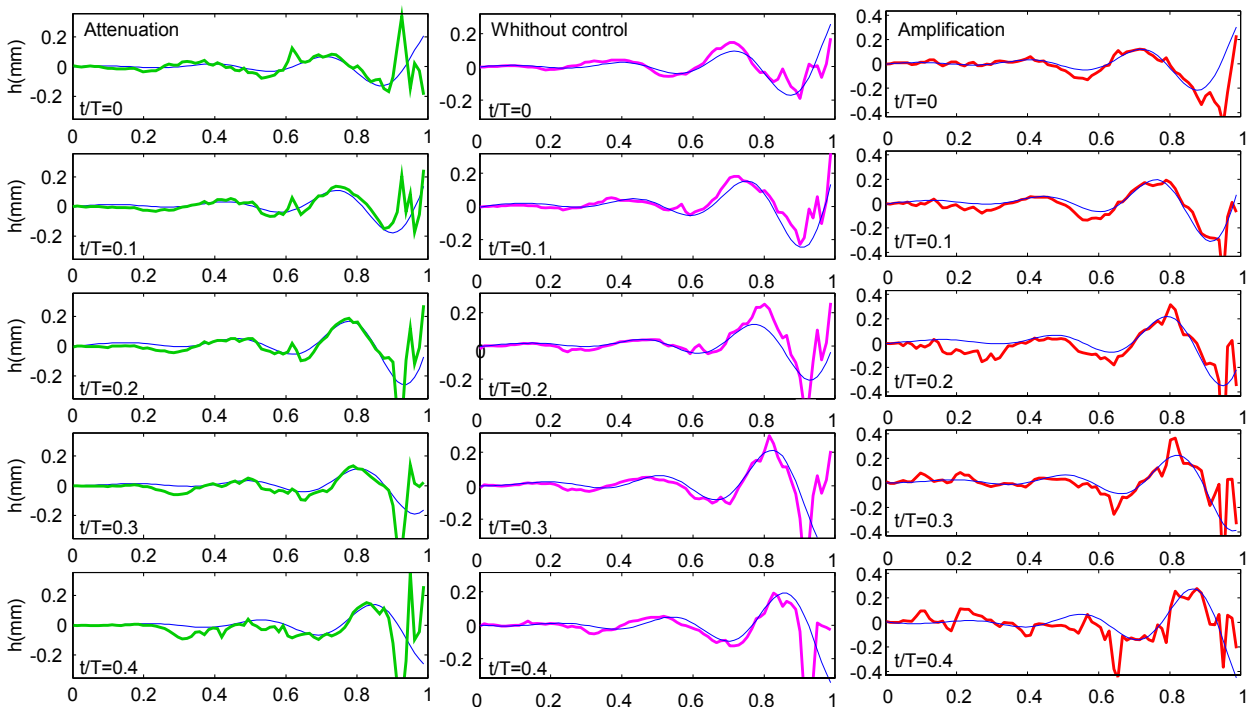


Figure 4: Effect of control on the oscillations of the mixing layer.

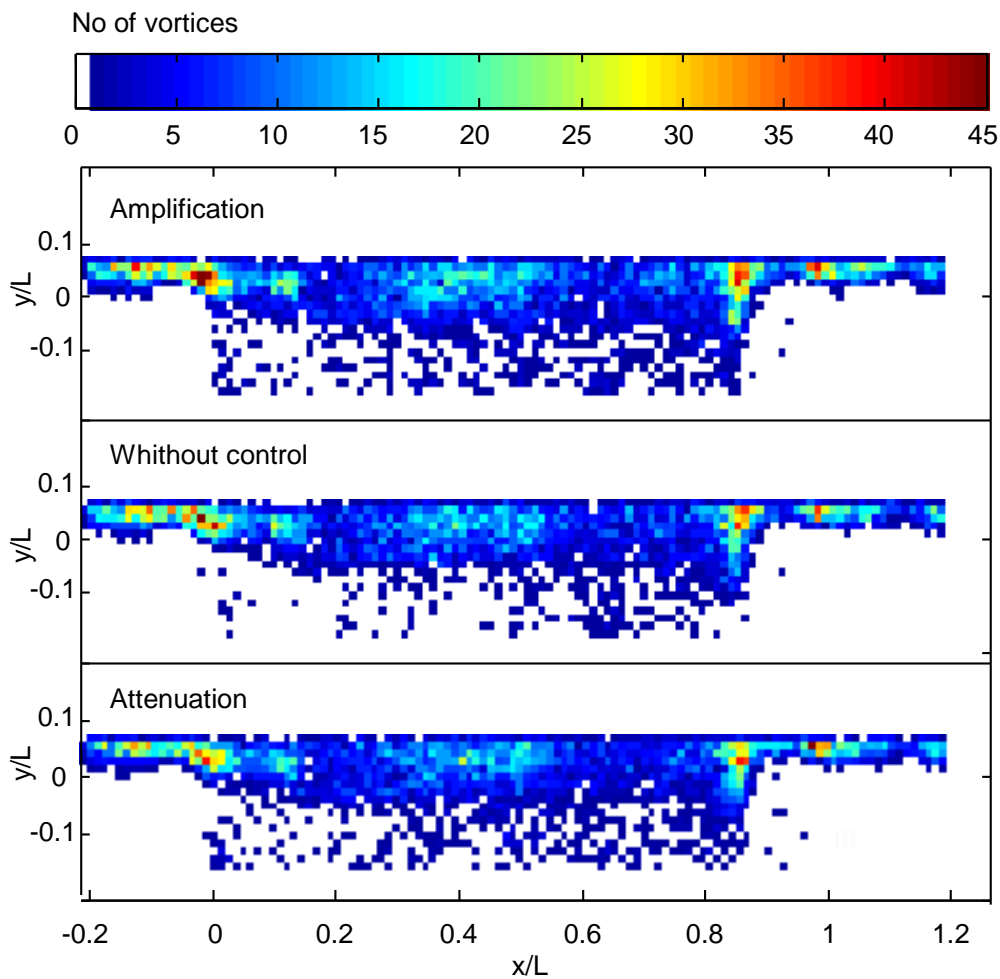


Figure 5: Total number of vortices detected in the cavity opening. Maps show the amplified, uncontrolled and attenuated cases.

The present analysis is focused on detection of small-scale vortical structures in order to assess the influence of active control on their growth and rate of production. The theoretical form of  $\lambda$  is used here. Results do correspond to phase-locked PIV measurements but are taken as an ensemble over the whole cycle. Thus, phase information is not taken as a parameter. Indeed, the decomposition of the cycle of oscillations in 10 equidistant time lags reveal no specific organisation in terms of vortical structures here. An overview of the distribution of vortices detected over a total of 1000 PIV fields per configuration is presented in Figure 5. An average of 6.6 vortices per velocity field are detected for the uncontrolled flow, whereas 6.7 and 6.8 vortices per velocity field are detected in the case of attenuation and amplification, respectively.

Qualitatively and quantitatively, few differences appear between the controlled and uncontrolled flows. The separation and impingement region see the greatest number of detected vortices and the depth at which vortices are detected grows as the mixing layer thickens, until the impingement region is reached. A significant number of vortices is also generated immediately upstream of the half length of the cavity. The main visible effect of control on the distribution of vortices is a slight increase of the number of vortices immediately below the mixing layer. This may be the result of

perturbations due to the propagation of sound waves generated by the actuator, which extent is  $0.2L$  below the downstream edge.

Figure 6 illustrates that control has no definite effect on the rate of production and dissipation of vortical structures, as the distributions of vortices along the cavity opening is very similar for controlled and uncontrolled flows. Most of the vortices generated in the vicinity of the separation point dissipate within the first fifth of the cavity length. As already shown in Figure 5, a significant number of vortices appear in the second fifth of the cavity before being dissipated between  $x/L=0.5$  and  $x/L=0.6$ . After a slight increase of production between  $x/L=0.6$  and  $x/L=0.8$ , the largest number of vortices is observable from  $x/L=0.8$  and  $x/L=0.9$ , which corresponds to a region of alternative clipping and shedding of vortices in cavity flows.

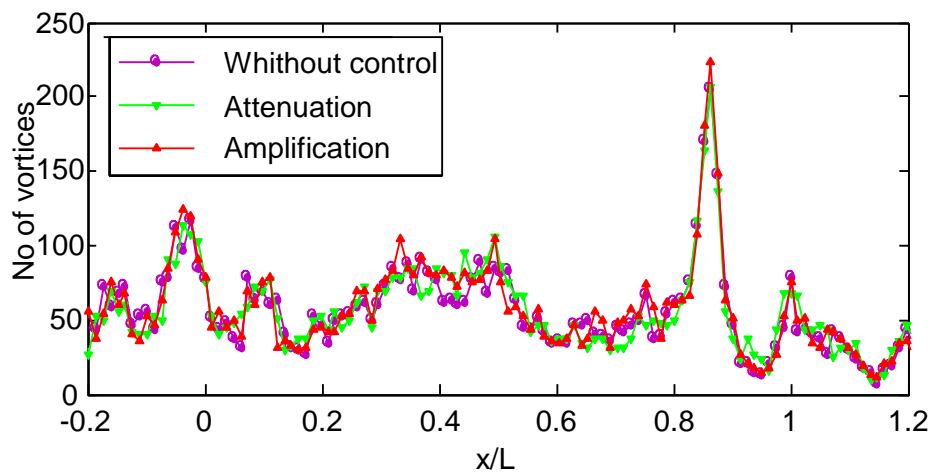


Figure 6: Total number of detected vortices in function of the longitudinal position

Statistics on the vertical position of detected vortices are presentend in Figure 7. The regions previously identified as dissipation regions correspond to zones where the mean position of vortices tends to drop towards the interior of the cavity, showing that dissipation actually occurs within the mixing layer. Inversely, in regions where vortices are generated, the mean vertical position tends to zero, indicating that production of vortical structures also logically takes place in the mixing layer.

Effect of control on the mean position of vortices consists in a slight displacement towards the interior of the cavity which can be observed from the separation region to the beginning of the impingement region. This displacement is slightly larger in the case of an amplification, especially in regions of transition between dissipation and generation of vortices.

Another effect of control on the distribution of vortices is shown by the RMS value of their vertical position. Logically, in the close vicinity of the downstream edge, strong interactions with the vibrating actuator occur, resulting in a higher variance of the position of vortices. More generally, this perturbation of the motion of vortices extends over the whole cavity opening, and particularly around  $x/L=0.7$  where perturbations of the oscillations of the mixing layer were already observed.

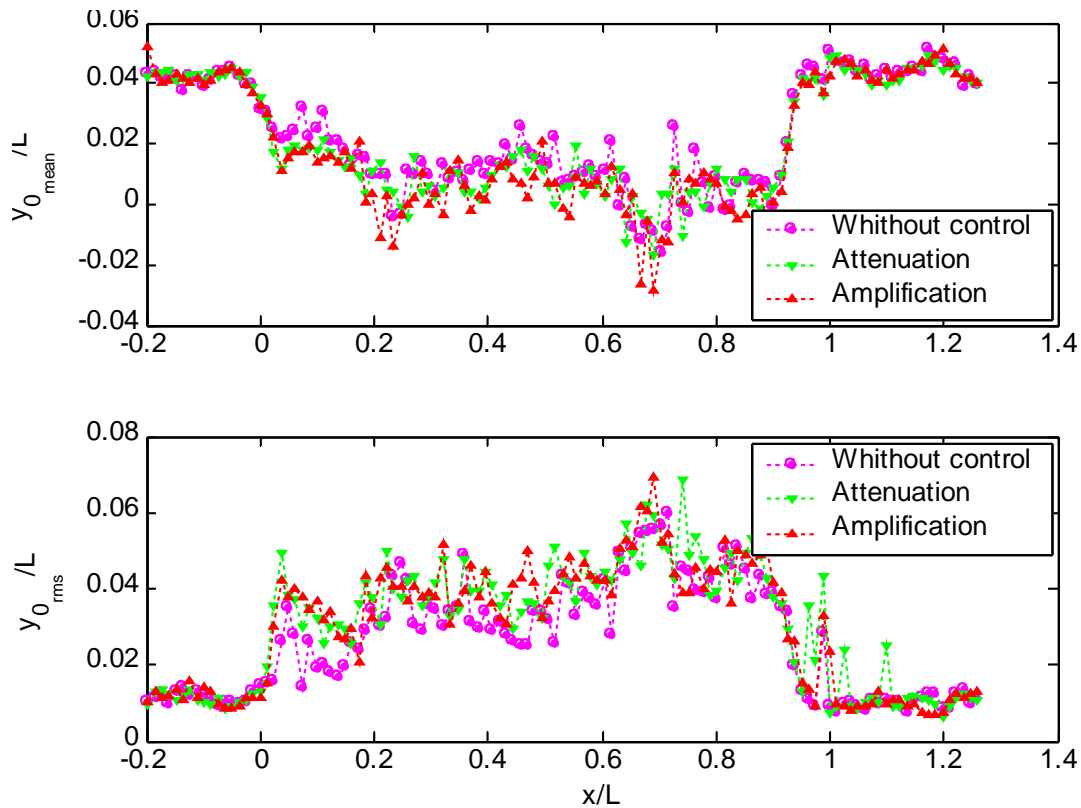


Figure 7: Mean and RMS vertical position of detected vortices in function of the longitudinal position.

The perturbations observed in the first part of the convective wave also appear in the distribution of vertical positions near the separation point. However, amplification and attenuation seem to have similar influence here, whereas the reconstructed motion of the mixing layer indicates that amplification has a greater perturbing effect than attenuation.

Statistics on the scale of detected vortices are presented in Figure 8. Since the theoretical  $\lambda$  form has been used here, vortices of radius smaller than half a grid cell (0.9 mm) clearly appear and shift results towards zero. As it is expected, regions of production of vortices show progressively increasing scales and regions of dissipation show decreasing scales. Again, effect of control can be observed in the region of influence near  $x/L=0.7$ .

Compared to the naturally oscillating flow, controlled flows exhibit a greater uniformity in the distribution of scales, which are also significantly smaller, at the exception of one measurement abscissa. Control also tends to enhance stability of the scale of vortices in this area, as shown by the distribution of RMS values. However, these observations must be cautiously interpreted as the measure of radii strongly deviates at small scales.



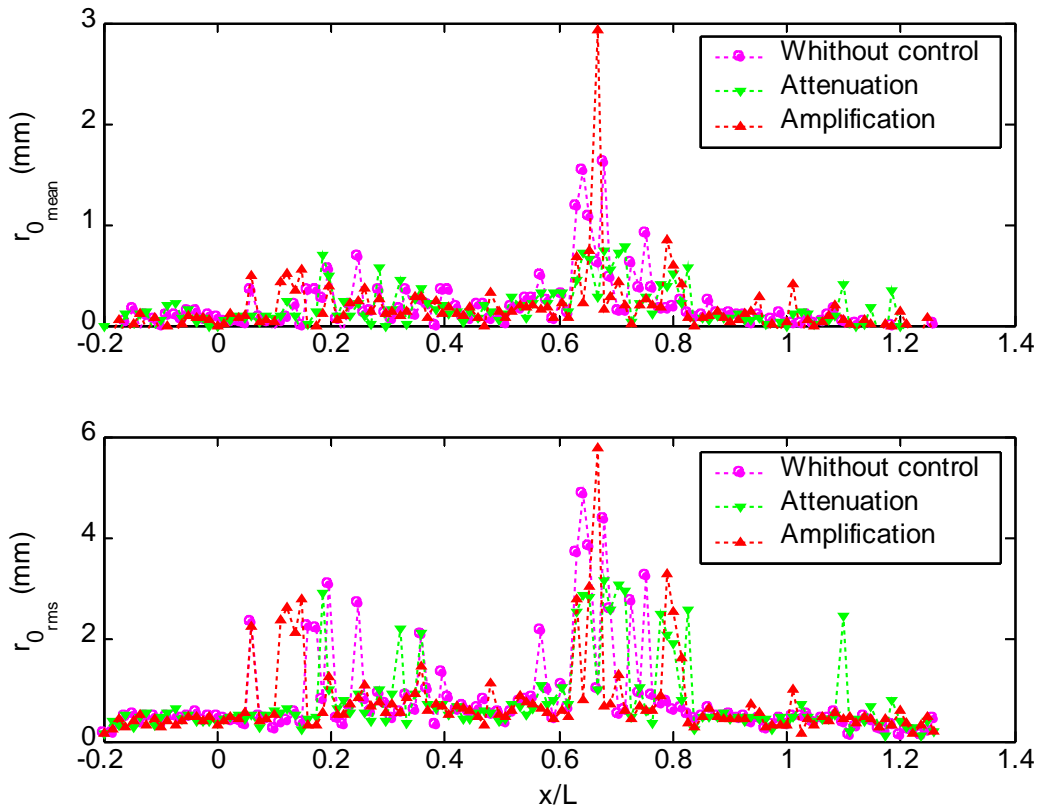


Figure 8: Mean and RMS scale of detected vortices as a function of the longitudinal position.

## 4 Conclusion

A detection algorithm based on scale-filtering of Jeong and Hussain's  $\lambda_2$  criterion in two dimensions is proposed in order to extract vortical structures at the scale of a PIV grid cell. Production, dissipation and primary characteristics of vortical structures convected in the mixing layer of a controlled cavity flow are investigated.

Results concerning the distribution of vortices over the cavity opening indicate that small-scale coherent structures are produced and diffused while being convected in the mixing layer. These are mostly generated in the impingement region, although a significant amount of vortices is generated at the separation point and, more generally, in the first half of the cavity opening, as it is commonly observed. However, these vortices are quickly diffused in the turbulent mixing layer and their number drops significantly over distances of the order of  $0.1$  to  $0.2$  cavity length. These results also indicate that control has no significant effect on the amount of vortices present in the mixing layer, but mostly influences their scale and motion. First, control slightly modifies the convection path of vortices and increases fluctuations of their vertical position. Second, control seems to reduce and stabilize the scale of convected vortices. However, this last interpretation cannot be fully validated given the limits of efficiency of the detection algorithm.

## References

- [1] J.E. Rossiter. Wind tunnel experiments of the flow over rectangular cavities at subsonic and transonic speeds. Aeronautical Research Council Reports and Memoranda, 3438, October 1964.
- [2] L. Chatellier, J. Laumonier, and Y. Gervais. Theoretical and experimental investigations of low mach number turbulent cavity flows. *Experiments in Fluids*, 36 :728–740, 2004.
- [3] E. Özsoy, P. Rambaud, A. Stitou, M. L. Riethmuller. Vortex characteristics in laminar cavity flow at very low Mach number. *Experiments in Fluids* 38:133–145, 2005.
- [4] L. Chatellier, J. Laumonier, and Y. Gervais. Theoretical and experimental investigations of low mach number turbulent cavity flows. *Experiments in Fluids*, 36 :728–740, 2004.
- [5] L. Chatellier, J. Laumonier, and Y. Gervais. Active control of the aeroacoustics of cavity flows from the downstream edge. *Comptes-Rendus Mécanique* 334:259–265, 2006.
- [6] A.A. Townsend. *The structure of turbulent shear flows*. Cambridge University Press, 1976